Preprint Cambridge Centre for Computational Chemical Engineering ISSN 1473 – 4273

How does blending oxygenated fuels affect soot formation from Jet A2 diffusion flames?

Yong Ren Tan [1,2], Maurin Salamanca [1,2,3], Jethro Akroyd [1,2], Markus Kraft [1,2,4]

released: July 6, 2021

[1] Department of Chemical Engineering
and Biotechnology
University of Cambridge
Philippa Fawcett Drive
Cambridge, CB3 0AS
United Kingdom

[2] CARES
Cambridge Centre for Advanced
Research and Education in Singapore
1 Create Way
CREATE Tower, #05-05
Singapore, 138602

[3] Escuela de Química, Facultad de Ciencias,
Universidad Nacional de
Colombia-Sede Medellín,
Calle 59 A No 63-20,
Medellín, Colombia.

[4] School of Chemical
and Biomedical Engineering
Nanyang Technological University
62 Nanyang Drive
Singapore, 637459

Preprint No. 274

Keywords: Smoke point, Sooting tendency, Laminar diffusion flame, Soot, Jet fuel, PODE, Oxygenated fuel

Edited by
Computational Modelling Group
Department of Chemical Engineering and Biotechnology
University of Cambridge
Philippa Fawcett Drive
Cambridge, CB3 0AS
United Kingdom

E-Mail: mk306@cam.ac.uk
World Wide Web: https://como.ceb.cam.ac.uk/

Abstract

Four oxygenated fuels: ethanol (EtOH), dimethyl carbonate (DMC), dimethoxymethane (DMM) and polyoxymethylene dimethyl ether ($PODE_3$) were blended with Jet A2 to investigate the sooting behaviour of the fuel mixtures. The smoke point was measured using wick-fed laminar diffusion flames as per the ASTM D1322 standard. The oxygen extended sooting index (OESI) was calculated to determine the sooting tendency of each mixture. Colour-ratio pyrometry and differential mobility spectrometry were used to measure the soot volume fraction (f_v) and particle size distribution (PSD). The addition of oxygenated fuels caused a strong reduction in sooting tendency (*i.e.* OESI) at low blend strengths (5%) and a weaker linear reduction at higher blend strengths (10% and 20%). Each mixture showed a similar reduction at a given mole fraction of oxygenated fuel. The OESI broadly correlated with the soot volume fraction and particle size measurements. Increasing blend strengths resulted in smaller particles at the tip of the flame. The average particle size at the tip was influenced by the oxygen content but not the molecular structure of the oxygenated fuels, whereas the soot volume fraction in the wings was influenced by both the molecular structure of the oxygenated fuels and the oxygen/carbon ratio of the mixture. For the first time, f_v and PSD have been reported for flames produced using Jet A2 blends in an ASTM D1322 lamp. The ability to relate data gathered using the ASTM D1322 standard for the sooting behaviour of different mixtures is going to be increasingly important as the aviation industry seeks to switch to sustainable fuels.

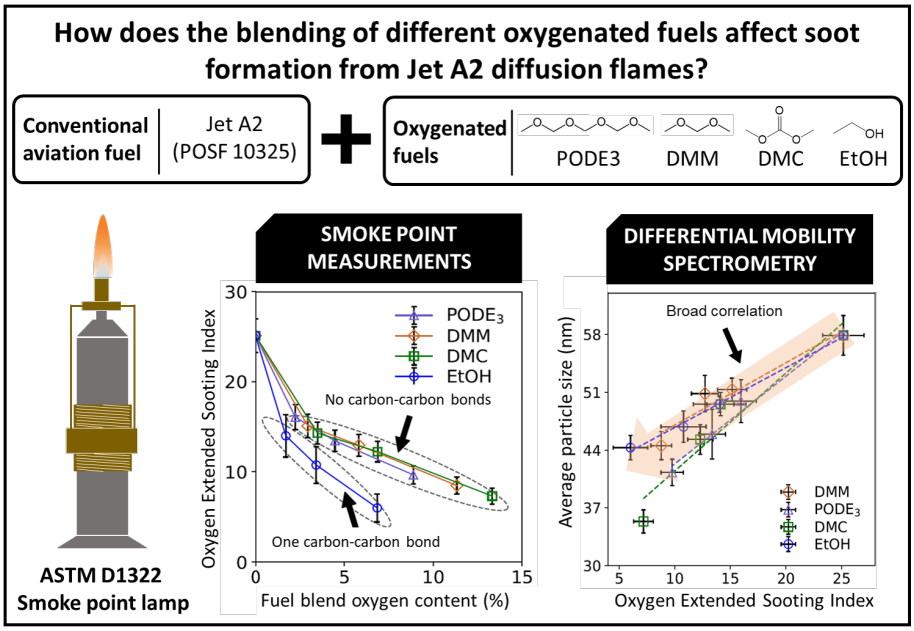

Highlights

- PSDs and soot volume fraction of Jet A2 flame were reported for the first time
- Good correlations of OESI with PSDs and soot volume fraction were observed
- Structural effect of oxygenated fuel important in determining sooting tendency

Contents

1 Introduction

Currently, the aviation industry accounts for approximately 15% of global oil demand [26]. Despite progress towards more sustainable alternative fuels, the oil demand from aviation is anticipated to keep growing until 2030 [26]. The combustion of fossil fuels derived from crude oil releases carbon dioxide, methane, soot, ultrafine particles ($PM_{0.1}$) and other pollutants, contributing significantly to climate change [54]. Soot [62] and ultrafine particles [9, 17, 41, 53] released into the atmosphere can alter cloud formation processes, causing changes in weather patterns and climate change. Human exposure to soot [37, 63, 81] and ultrafine particles [17, 22] can have adverse health implications. Ultrafine particles can deliver toxic semi-volatile coatings to human brains by penetrating our respiratory tract [17, 22]. Notably, particulates contributing to air pollution from the combustion of fuels can link to COVID-19 related deaths [61, 84, 103]. There is a clear need to move away from harmful unsustainable fuels [47–50].

Despite the relative ease of electrification for land transportation, Conventional Aviation Fuel (CAF), derived from fossil fuels, remains the prominent means of powering the aviation industry [90] because of the high energy density of liquid fuels [47]. The International Civil Aviation Organisation (ICAO) announced a vision to replace CAF with Sustainable Aviation Fuel (SAF) by 2050 to lower the carbon footprint of the aviation industry [36]. Only a few SAFs are currently approved for commercial aircraft engines [5]. The approved SAFs are composed of a mixture of hydrocarbons sourced from hydroprocessed esters, fatty acids and alcohols [5].

The performance of aircraft engines is sensitive to the properties of the fuels, and stringent regulations govern the quality of the fuel blends [34]. This includes the specific energy, energy density, thermal stability and emissions, the operability (freeze point, density, viscosity and reactivity) and drop-in compatibility (infrastructural compatibility) of the fuel [34]. To meet these requirements and minimise the change in the quality of the resultant fuel blend, only low volumes (up to 50%) of SAFs can be blended with CAFs [34]. In practice, commercial SAFs are blended with CAFs at less than 10 vol.% due to the high cost and constrained supply of the feedstock to produce SAF [27, 34, 71, 90].

Another approach to using SAFs in the aviation industry is by directly blending sustainably sourced esters, fatty acids and alcohols (*i.e.* without subsequent conversion to hydrocarbon fuels) with CAFs [5]. Esters, fatty acids and alcohols are also known as oxygenated fuels due to the oxygen present in their molecular structure [50]. Ethanol (EtOH) [57, 80], dimethoxymethane (DMM) [48], poly(oxymethylene) dimethyl ethers (PODE) [6, 8, 25, 48, 58, 59] and dimethyl carbonate (DMC) [1, 49, 55, 99] are all examples of oxygenated fuels that have been identified as promising candidates for SAFs [102].

Many fundamental experimental studies on the formation of soot and soot precursors involving EtOH have been reviewed [50, 80]. DMM, PODE [48], and DMC [1, 49, 85] have been more recently proposed as clean fuels because of their high oxygen content and the absence of carbon-carbon bonds in their molecular structures. It is thought that these features may contribute to a reduction in the formation of soot precursors. Generally, the molecular structures of the oxygenated fuels are highly related to the formation of hazardous regulated and unregulated emissions during combustion [48, 50, 80]. The

understanding of the emission properties of jet fuel blended with oxygenated fuels is consequently an ongoing subject of research to evaluate the relative benefits of such a strategy.

The blending of oxygenated fuels with jet fuels is effective in reducing soot formed in engines [52, 67, 68]. In an aircraft engine, the use of oxygenated fuel-jet fuel blends reduced the number, the size and the mass of the particulate emissions [67]. Moreover, the composition of the blends and the thrust of the engine was found to influence the nanostructure of the soot [52]. This highlights the complexity of disentangling the effect of the operations of the engine from the effect of the blending of the oxygenated fuels [68]. Laboratory flame studies can be an effective means to evaluate the blending effects of oxygenated fuels with jet fuel under controlled combustion conditions [83].

Laminar laboratory flames have been used in the literature to compare the effect of different oxygenated fuels on the formation of soot and soot precursors when blended with hydrocarbon fuels [14, 15, 40, 42, 43, 45, 46, 56, 57, 64, 65, 70, 76, 78, 79, 82, 88, 91, 98, 100, 104]. Two of the most commonly studied class of oxygenated fuels in flames are alcohols and ethers. The blending of EtOH with hydrocarbons was found to reduce the soot volume fraction of laminar diffusion flames [57] and premixed flames [77]. Similarly, *n*-butanol blends in n-dodecane showed a reduction in soot particle mass with increasing *n*-butanol concentration in laminar premixed flames [30]. When EtOH and *n*-butanol blends with iso-octane were compared in laminar premixed flames, *n*-butanol was found to induce a stronger soot reduction than EtOH [29]. However, a comparison between EtOH and methanol showed more complex behaviour in ethylene counterflow diffusion flames [100]. Methanol was observed to reduce the formation of soot at all blend strengths, whereas EtOH increased the formation of soot at low blend strengths and reduced the formation of soot at high blend strengths [100]. This was attributed to the fact that methanol decomposes to form CO which reduced the proportion of carbon from the fuel that contributed to soot formation, whereas EtOH decomposes to form methyl radicals which were hypothesised to activate a C1+C2 route that enhanced soot precursor formation at low blend strengths before reducing the overall rate of soot formation at high blend strengths [100]. The observations do not show a clear trend in terms of which alcohol produces the highest reduction in the formation of soot. The relative soot suppression by the alcohols varied depending on the type of the base fuel and the blend strength.

Comparisons of oxygenated fuel isomers were conducted by investigating the behaviour of butanol isomers in laminar premixed flames where the formation of soot precursors [70, 79] and the resultant particle size distribution [76] were found to be influenced by the molecular structure of the isomers. The formation of soot precursor (benzene) was found to be highly dependent on the specific isomeric fuel. The *tert*-butanol flame formed the highest level of benzene, followed by *iso*-butanol, 2-butanol and 1-butanol. The formation of benzene was identified to be related to the formation of propargyl radicals from the decomposition of the butanol isomers [70]. When the EtOH and dimethyl ether (DME) isomers were compared, they showed a similar reduction in the formation of soot precursors in premixed *n*-pentane flames [40]. Interestingly, a small amount of DME was found to enhance the formation of soot more than EtOH in laminar coflow diffusion ethylene flames. This was shown to be because DME produces more methyl radicals than EtOH during fuel decomposition in the flame [64]. In a non-premixed counterflow flame, DME/*n*-heptane blends showed a significant reduction in soot precursors

because the methyl radicals formed from DME were unable to contribute effectively to the growth of soot precursors [98]. These investigations demonstrate that the oxygenated fuel-structure-specific chemistry affects the formation of soot precursors and soot.

The ASTM D1322 standard specifies a test methodology for the characterisation of the sooting tendency of jet fuels using laboratory wick-fed laminar diffusion flames to measure the smoke point (SP) [5]. The SP is defined as the maximum flame length of a smokeless flame. Notwithstanding the standardisation of the methodology to gauge the quality of jet fuels based on their sooting tendency, it fails to provide crucial information about the characteristics and the properties of the emissions such as the size, the mass and the concentration of the particulates. The importance of these characteristics is evident from a recent announcement by the ICAO, which will introduce new standards regarding the regulation of the mass and the number of particulate emissions for the engines of aircraft [74]. Some investigations have sought to correlate the measurements of the sooting tendency of the oxygenated fuels in diesel blends with the engine particulate emission [32, 33] and soot volume fractions [93] using ASTM D1322 SP lamps. Nevertheless, information about the correlation of measurements made using a SP lamp with the size of particulates is a gap that needs to be addressed, particularly considering the negative impact of ultrafine particles ($PM_{0.1}$) on the environment and health [9, 17, 22, 41, 53].

Many research groups have investigated the sooting behaviour of oxygenated fuels. However, it remains unclear which aspects of the fuels are most important in influencing the sooting behaviour. The structure of the molecules [33, 38, 73], bond saturation [32], oxygen content [24, 60] and the oxygen-containing functional groups [32, 38, 73] have all been shown to influence the sooting tendency. In SP lamp studies of oxygenated fuels blended with diesel, the effect of the 'dilution' of the diesel with the oxygenated fuel was found to have the largest influence on soot reduction. However, the oxygen content of different oxygenated fuels was not able to explain all of the difference in the observed soot suppression behaviour and different oxygenated functional groups were observed to cause significant differences in soot suppression behaviour [87]. Despite some improvements in understanding the factors that affect the sooting tendency of different oxygenated fuels, the relationship between sooting tendency and the quantities of practical value (*i.e.* particle size distribution and soot volume fraction) remains poorly understood.

The **purpose of this paper** is to measure the sooting tendency of different oxygenated fuel-jet fuel blends using the standard ASTM smoke point lamp and to measure, analyse, and correlate the corresponding particle size distribution and soot volume fraction of the fuel mixtures. The analysis and correlations of the data will facilitate the understanding of the implications of using different oxygenated fuels that have been identified as promising candidates for SAFs, which can have practical value and relevance to the aviation industry.

2 Materials and methods

A smoke point (SP) lamp was used to investigate laminar diffusion flames using liquid fuel blends. The SP was measured to provide an estimate of the sooting tendency of each fuel mixture. A quartz sampling probe connected to a Cambustion DMS500 Differential Mobility Spectrometer was used to measure the particle size distribution at the tip of the flame. A Blackfly S colour camera was used to image the flames and an in-house Python code [19] used to perform Abel inversion on the flame images to compute the soot volume fraction measurements. **Figure 1** shows a schematic of the experimental setup.

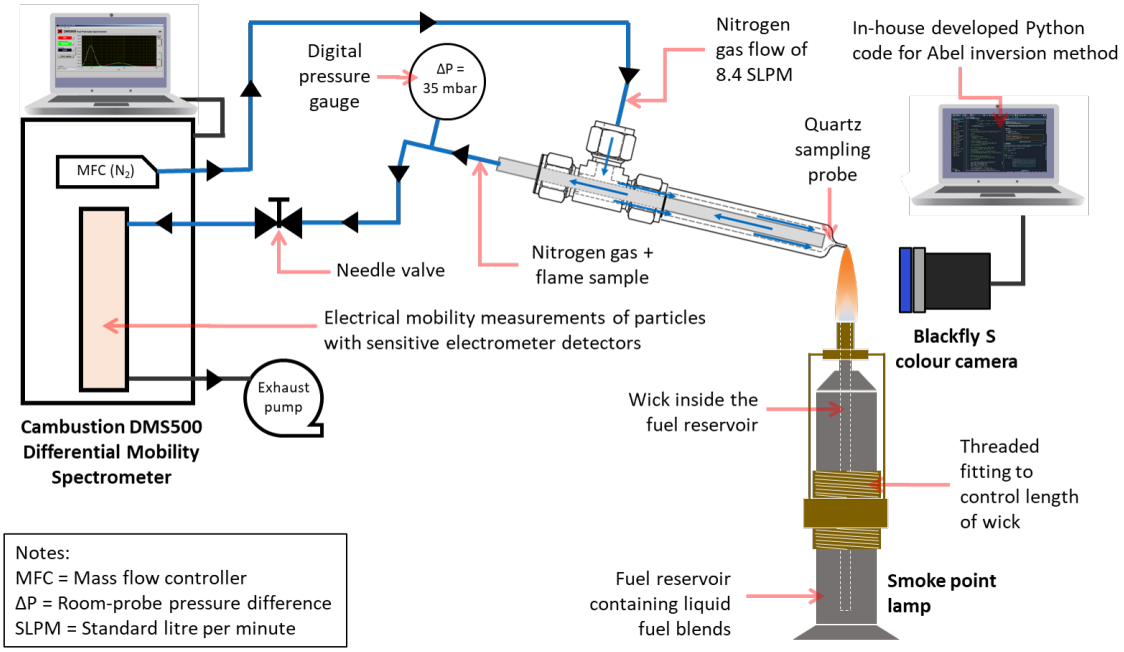

Figure 1: *Schematic of the experimental setup.*

Thirteen fuel mixtures were investigated. The base fuel was a Jet A2 (POSF 10325) conventional kerosene [72] obtained from the United States National Jet Fuel Combustion Program (NJFCP) [16]. NJFCP has reported the detailed chemical composition and physical properties of Jet A2 [16]. The Jet A2 was blended at 5%, 10% and 20% by volume with poly(oxymethylene) dimethyl ether ($PODE_3$), dimethyl carbonate (DMC), dimethoxymethane (DMM) and ethanol (EtOH). The $PODE_3$ was procured from ASG Analytik-Service GmbH with a purity of 95%, while DMC, DMM and EtOH were procured from Tokyo Chemical Industry UK Ltd with a purity of at least 95%. They were used without further purification. The fuel blends were miscible without phase separation over time. This is important because phase separation indicates an incompatibility of the oxygenated fuel blending percentage with the hydrocarbon fuel [39].

2.1 Smoke point and sooting indices

Typically, the smoke point (SP) is measured using a standardised ASTM D1322 procedure involving flames generated using a standard ASTM D1322 SP lamp [4]. The SP is defined

as the flame height at which smoke is first observed to escape from the tip of the flame, where the height of the flame can be controlled by adjusting the exposed length of the wick of the SP lamp. The SP measurements enable the quantification of the sooting tendency of liquid fuels [4], where the SP is inversely proportional to sooting tendency [4, 69].

The Threshold Sooting Index (TSI) enables a comparison of the sooting tendency of different hydrocarbon fuel blends on a unified scale that is independent of the SP apparatus [2, 10–12, 21, 35, 75]. The TSI provides an experimentally-obtained correlation with the SP [69] that is directly proportional to the molecular weight (MW) and inversely proportional to the SP of the fuel [13]. It has been shown to correlate with the molecular structure of the fuel molecules through structural group contributions, and can be useful in determining the sooting tendency of hydrocarbons and assist in the formulation and evaluation of fuels [101].

Nevertheless, TSI fails to consider the presence of oxygen in blends of hydrocarbons with oxygenated fuels. This is important because the oxygen in the fuel reduces the amount of oxygen required for stoichiometric combustion [7, 13]. Hence, an analogous quantity, known as the Oxygen Extended Sooting Index (OESI), was introduced to take the additional oxygen into consideration [7]

$$\mathrm{OESI} = a_{\mathrm{OESI}} \left(\frac{n + \frac{m}{4} - \frac{p}{2}}{SP} \right) + b_{\mathrm{OESI}}, \tag{1}$$

where n, m and p are the amount of carbon, hydrogen and oxygen in a fuel mixture with a generic fuel with mean formula $C_nH_mO_p$. The evaluation of OESI requires the calibration of the a_{OESI} and b_{OESI} constants for each experimental setup. Currently, OESI is widely used in the literature to evaluate the sooting tendency of fuel blends containing oxygenated fuels [32, 33, 38, 87].

In this work, we used a modified SP lamp that is equipped with a threaded fitting to adjust the exposed length of the wick and hence flow rate of the fuel in the wick-fed flame. The modified SP lamp has been described in detail previously [87, 96]. We followed the ASTM D1322 [4] procedure to measure the SP of each fuel mixture. All SP measurements were repeated five times to obtain an average SP. The SP lamp was calibrated by measuring the SP of 2,2,4-trimethylpentane and toluene as reference fuel blends as per ASTM D1322 [4]. The OESI constants a_{OESI} and b_{OESI} were calibrated using 1-methylnapthalene, n-heptane, decane, toluene, cyclohexane and dodecane as reference fuels. The SPs of these reference fuels were measured and a_{OESI} and b_{OESI} computed to reproduce the defined OESI values for the reference fuels, where the OESI of n-heptane and 1-methylnapthalene were assigned values of 2.6 and 91 respectively to normalise the OESI scale in accordance to the procedure reported in the literature [7, 69]. The a_{OESI} and b_{OESI} constants were computed to be 38.7 ± 4.0 and -6.2 ± 0.7, respectively. The error of the OESI was computed using the error propagation method reported previously [96].

2.2 Flame lengths and fuel flow rates

The flame lengths were adjusted to about 24.5 mm for all flames during colour-ratio pyrometry and differential mobility spectrometry measurements. The chosen flame length

is 0.5 mm below the SP of Jet A2, where Jet A2 has the lowest SP of all the fuel blends studied, similar to the procedure reported in the literature [93]. This approach is necessary to ensure that all the flames have a closed-tip for reliable soot volume fraction and particle size distribution measurements [93].

Figure 2 shows the fuel flow rates of the flames with a fixed flame length of 24.5 mm. The fuel flow rates are within ±10% deviation of the Jet A2 flame. The fuel consumption of each flame is reported in **Table A1.2**. The measurements were logged using a Precisa Series 320 XB analytical balance with a readability of 10 mg.

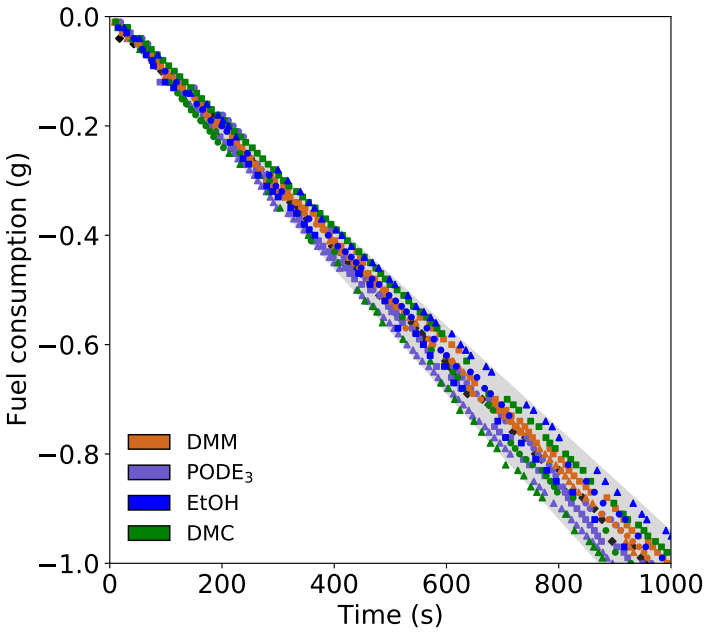

Figure 2: *The fuel consumption of the oxygenated fuel-jet fuel blend flames measured over 1,000 seconds. The volumetric blending percentages of oxygenated fuel are 0 vol.% (◇), 5 vol.% (□), 10 vol.% (○) and 20 vol.% (△). The grey shaded region shows ±10% deviation of the fuel consumption measured for the Jet A2 flame.*

2.3 Colour-ratio pyrometry

Colour-ratio pyrometry was used to measure the soot volume fraction (f_v) of the flames [19, 51]. The measurement system has been described in detail previously [19, 88, 89]. The image processing and soot volume fraction computations were executed using an in-house Python code [19] using the BASEX Abel inversion method [3, 20] which is available online [18].

2.4 Differential mobility spectrometry

Typically, flames involving real fuels generate particles with a broad range of particle sizes [66]. Hence, in the current work, we selected the Cambustion DMS500 Differential Mobility Spectrometer to measure the particle size distribution (PSD) of the particles. The Cambustion DMS500 allows the measurement of a broad range of particles sizes, from 5 nm up to 2,500 nm, enabling measurement of the full particle size distribution (above 5 nm) in the Jet A2 and blended flames. A quartz sampling probe with a needle valve is connected to the Cambustion DMS500 for PSD measurements at the tip of the flame, as shown in Figure 1.

Our previous work has described in detail the sampling procedure and the calibration and calculation of the dilution ratio [88, 89]. In brief, we performed the sampling at the tip of the flame with an input nitrogen dilution flow of 8.4 SLPM and a room-probe pressure difference of ΔP = 35.0 mbar. The data reported for each flame are an average of five repeat measurements. The measurements were performed at the tip of the flame because it avoids the clogging of the probe and the issue of flame perturbation that would compromise the quality of the measurements when sampling inside the wick-fed diffusion flames. The current choice of sampling point has been shown to provide a strong measurement signal and meaningful results [10–12].

3 Results and discussion

In this section, the results of the oxygen extended sooting index (OESI), soot volume fraction (f_v) and particle size measurements of the oxygenated fuel/Jet A2 wick-fed laminar diffusion flames are discussed in detail. The correlations of the average particle size and soot volume fraction of the flames with the oxygen/carbon ratio and the OESI of the fuel blends are investigated and explained.

3.1 Sooting propensity of oxygenated fuel blends

Figure 3(a) and **(b)** show the smoke point (SP) measurements as a function of the volumetric percentage and mole percentage of the oxygenated fuel in the Jet A2 blends, respectively. The smoke point (SP) measurements of all the fuel blends are reported in **Table A1.1**. The standard error of the SP measurements over five repeats are reported as error bars. The Jet A2 flame was determined to have a SP of 25.0 mm, consistent with the literature value [23].

There is a positive correlation between the SP and the proportion of the oxygenated fuels in Jet A2. It is clear that the addition of the oxygenated fuels suppresses the formation of soot in the flame. Figure 3(a) shows no significant differences between the oxygenated fuel blends relative to the size of the error bars at each volumetric blend strength. However, Figure 3(b) shows that differences can be observed between the oxygenated fuel blends at the same mole percentage. Among all the oxygenated fuels, $PODE_3$ is most effective at reducing the sooting tendency when blended with Jet A2, followed by DMC,

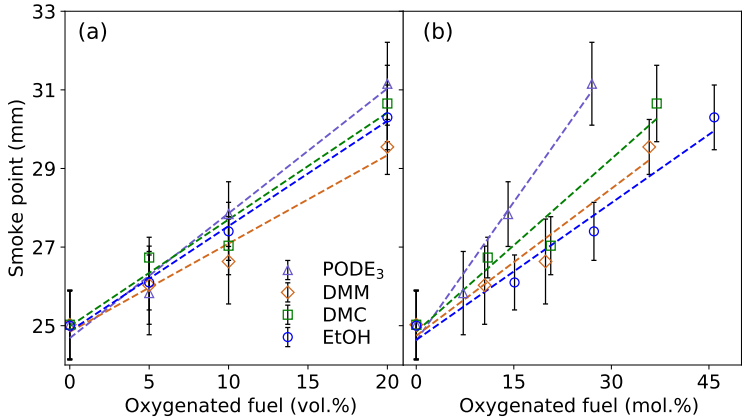

Figure 3: *The smoke point of the flames against the (a) volumetric percentage and (b) mole percentage of the oxygenated fuel-Jet A2 blends. The dotted lines correspond to the best fit to the data for each oxygenated fuel-Jet A2 blend to guide the eye. The error bars show the standard error of the smoke point measurements over five repeats.*

DMM and EtOH. The differences between the SP of the oxygenated fuel blends broadens as the mole percentage of the oxygenated fuel in the blend increases.

The trend is related to and reflected in the molecular weight (MW) of the oxygenated fuels. The change in the MW of the oxygenated fuel alters the amount of oxygen required to diffuse into the flame for complete combustion of one mole of the fuel [13]. Consequently, the flame length and SP will be affected. $PODE_3$ (MW = 136 g/mol), which has the largest MW amongst the oxygenated fuels studied has the largest increase in the SP, followed by DMC (MW = 90 g/mol), DMM (MW = 76 g/mol) and EtOH (MW = 46 g/mol). The broadening of the SP measurements between the fuel blends is due to the increasing influence of the MW of the oxygenated fuels at increasing blend strength. Notably, the importance of considering the differences in the MW (and the molecular structure) of the fuels in understanding the sooting tendency has been highlighted and verified [101]. The SP measurements do not account for the molecular composition of the fuel blends [13] and, for this reason, subsequent analyses are performed using OESI in place of SP [7, 13].

Figure 4(a), (b) and (c) show the OESI of the flames against the volumetric percentage, mole percentage and the oxygen content of the fuel blends respectively. The error bars show the error calculated using the error propagation method reported previously [96]. Figure 4(a) and (b) show that low blend strengths (5 vol.%) of the oxygenated fuels cause a strong reduction in sooting tendency (*i.e.* OESI). At higher blending strengths (10 vol.% and 20 vol.%) of the oxygenated fuels, a weaker linear reduction in sooting tendency is observed. Interestingly, the data in Figure 4(b) is grouped more tightly than Figure 4(a). The first observation suggests that significant suppression of the soot can be achieved even with low blend strengths of oxygenated fuels. The second observation suggests that increasing the blend strength of oxygenated fuels with Jet A2 could be used to further decrease the sooting tendency (*i.e.* OESI).

Figure 4(c) shows the OESI plotted against the oxygen content of fuel mixtures. It is ob-

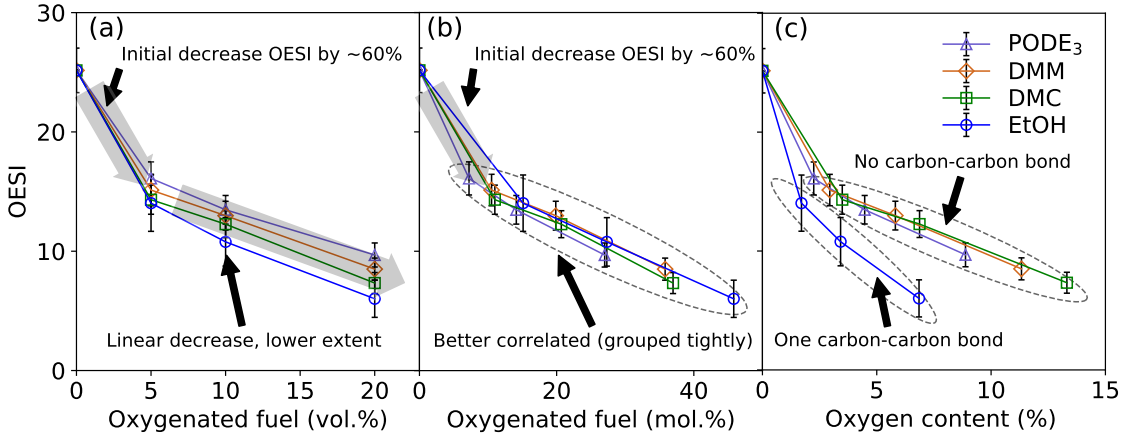

Figure 4: *The oxygen extended sooting index (OESI) of the flames against (a) volumetric percentage (b) molar percentage and (c) the oxygen content of the fuel blend. The error bars show the error calculated using an error propagation method [96].*

served that the fuel blends with DMM, $PODE_3$ and DMC have OESIs that are tightly correlated. They have similar molecular structures, *i.e.* rather than having carbon-carbon (C-C) bonds, they have carbon-oxygen-carbon (C-O-C) bonds where the oxygen-containing functional groups are embedded within their skeletal structures. However, EtOH has a distinctively different structure from DMM, $PODE_3$ and DMC. EtOH contains a C-C bond and has an oxygenated functional group that is not embedded within its skeletal structure. These observations suggest that whilst the oxygen content of the fuel blend correlates with the reduction in sooting tendency, it is not the sole factor. The effect of the molecular structure is also important in understanding the sooting tendency of the fuel blends.

This result is consistent with the trend in the formation of soot precursors among dimethyl ether (DME) [95], diethyl ether (DEE) [92], and di-*n*-butyl ether (DBE) [97]. DME (no C-C bond), DEE (two C-C bonds), and DBE (six C-C bonds) are mono-ethers with a different number of C-C bonds in their molecular structures. The increase in the concentration of specific soot precursors in the mono-ether flames was found to be correlated with the increase in the number of C-C bonds in the mono-ethers [92, 95, 97]. The increased number of C-C bonds in the mono-ethers was shown to affect the mono-ether fuel decomposition pathways and hence the distribution of the soot precursors formed.

In short, the oxygen content of the fuel blend, the chemistry of the oxygen-containing functional group and the molecular structure of the oxygenated fuel can have important contributions to the change in sooting tendency. More importantly, we have found that the effect of the C-C bond in the skeletal structure and the chemistry of the oxygen-containing functional group may have a stronger effect on sooting tendency than the oxygen content of the fuel blends.

3.2 Soot volume fraction of oxygenated fuel blends

Figure 5 shows the spatial distribution of the soot volume fraction, f_v, obtained from colour-ratio pyrometry of the flames. The mixture strength (volumetric percentage of oxygenated fuels in Jet A2) is indicated at the top of each image. The maximum soot volume fraction in the wing of the flame is indicated at the bottom of each image. This discussion focuses on the maximum soot volume fraction which occurs in the wing of the flame [93]. In addition, it is noted that colour-ratio pyrometry works best in optically thin flames, and that the values of the soot volume fraction in the wings (optically thinner) will have better resolution than at the centre-line of the flame (optically thick) [19, 44]. There are no comparable values of the soot volume fraction of jet fuel flames in a SP lamp available in the literature. However, in the current work, the observed values of the soot volume fraction values (0–10 ppm) are consistent with soot volume fraction values (0–12 ppm) of biodiesel/diesel flames in a SP lamp measured using laser-induced incandescence [93].

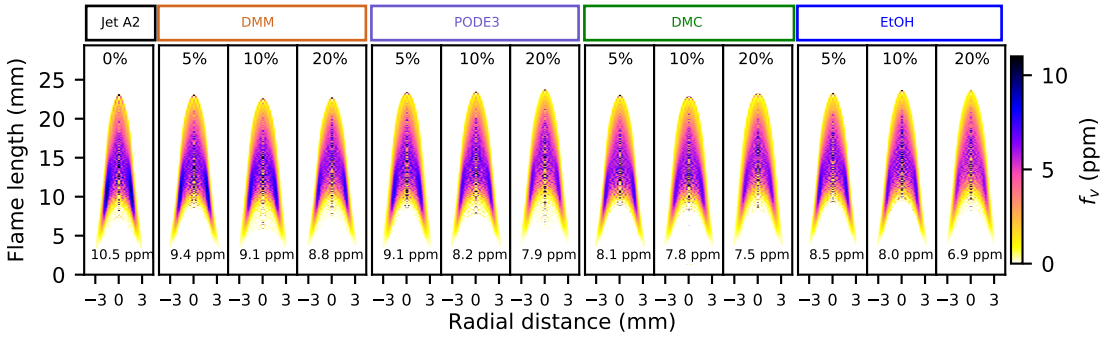

Figure 5: *The soot volume fraction, f_v, of the oxygenated fuel-Jet A2 blend flames. The percentage of DMM, PODE$_3$, DMC and EtOH in each fuel blend is indicated at the top of each image. The maximum f_v in the wing of the flame is indicated at the bottom each flame.*

The Jet A2 flame was observed to have a maximum soot volume fraction of 10.5 ppm in the wing, which was the highest of all the flames studied. The maximum soot volume fraction in the wing of the flame is observed to decrease as the proportion of the oxygenated fuels in the fuel mixture increases. EtOH showed the lowest soot volume fraction, followed by DMC, PODE$_3$ and DMM for the fuel mixtures with 20% oxygenated fuels. The discussion of the trend will be covered in **Section 3.4**.

There are three key takeaways from the observations in Figure 5. Firstly, the blending of the oxygenated fuels with jet fuel reduces the production of the soot. Secondly, the degree of the reduction of the soot volume fraction is dependent on the types of the oxygenated fuels involved in the blending. Thirdly, EtOH causes a greater reduction in the soot volume fraction than DMC, DMM and PODE$_3$.

3.3 Soot particle size distribution of oxygenated fuel blends

Figure 6 shows the particle size distribution (PSD) at the tip of the flames. The standard errors of that PSDs are reported as error bars over five repeats. To the best of the authors' knowledge, this is the first time the PSDs at the tip of the flame have been reported in the literature for this flame configuration using jet fuel blended with oxygenated fuels. Comparable data are therefore not available for the current measurements.

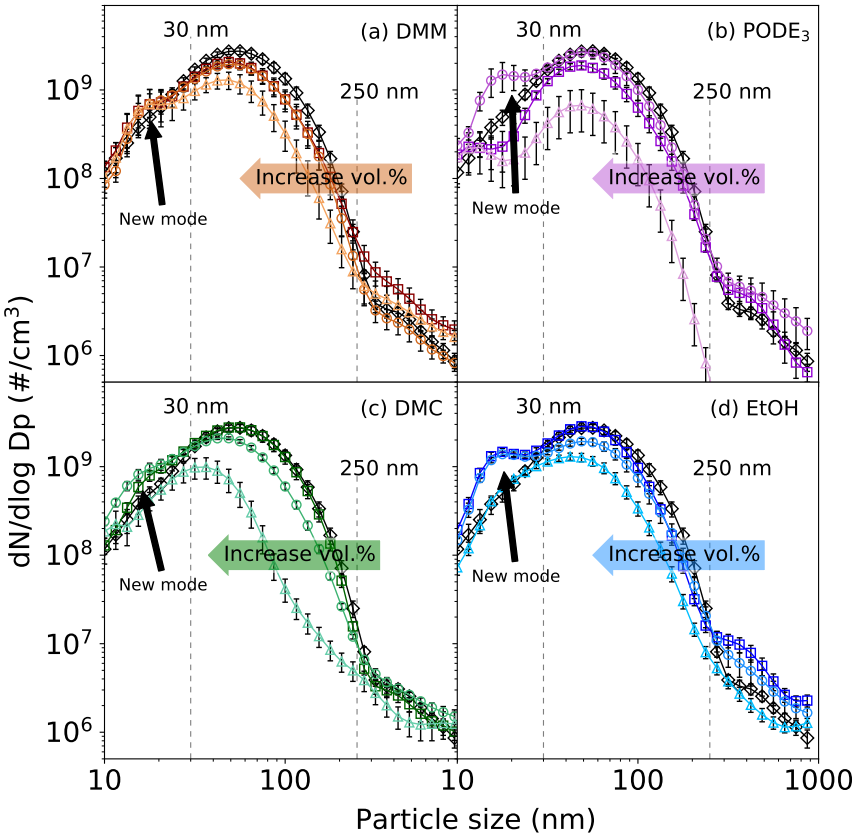

Figure 6: *The particle size distributions (PSDs) at the tip of the flame for the oxygenated fuel-Jet A2 blend flames. The volumetric blending percentages of the oxygenated fuels are 0 vol.% (◇), 5 vol.% (□), 10 vol.% (○) and 20 vol.% (△). The dotted vertical lines indicate particle sizes of 30 nm and 250 nm, while the horizontal arrows indicate the shift to smaller particle sizes at higher blend strengths. The error bars show the standard error of the measurements at the tip of the flame tip over five repeats.*

As the blend strength of the oxygenated fuels increases (so inducing a decrease in sooting tendency), there is a change from unimodal to bimodal PSDs and a shift towards smaller particle sizes. The additional mode appears on the left of the PSDs in the size range 10 nm to 30 nm. Notably, DMC and $PODE_3$ exhibit a larger change in the PSDs than DMM and EtOH with increasing blend strengths. This change is also observed in the larger particle sizes. The effect was strongest in the 20% $PODE_3$ blend, which showed no particles larger than 250 nm.

These observations show that high proportions of oxygenated fuels in Jet A2 can move the particle size distribution towards small particles, increasing the proportion of ultrafine particles ($PM_{0.1}$) formed during combustion. These particles can be harmful to health and the environment [9, 53]. The differences between the PSDs observed for oxygenated fuels suggests that the proportion of oxygenated species in flame can influence the particle formation process in the flames, where the oxygenated fuels with high oxygen/carbon (O/C) ratio ($PODE_3$ and DMC at 1.1 and 1.3 respectively) have larger change in their PSDs than oxygenated fuels with lower O/C ratio (EtOH and DMM at 0.7 and 0.9, respectively).

3.4 Correlations of soot measurements to fuel blend oxygen/carbon ratio

Figure 7(a) shows the percentage decrease in the soot volume fraction in the wings of the flames versus the oxygen/carbon (O/C) ratio of the fuel mixtures.

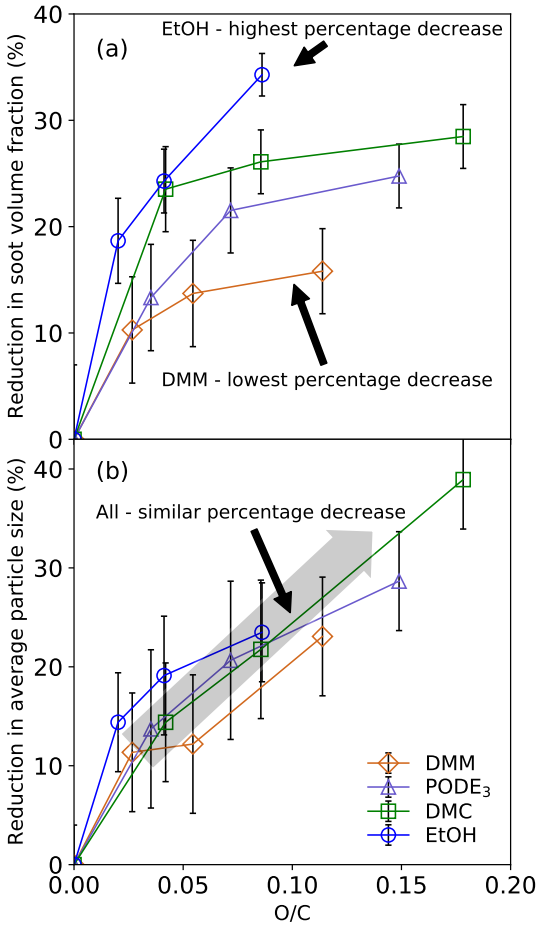

Figure 7: *The percentage reduction in (a) maximum soot volume fraction in the wing of the flame and (b) average particle size at the tip of the flame versus the oxygen/carbon (O/C) ratio of fuel blends. The error bars show the standard error of the measurements over five repeats.*

The increase in the O/C ratio of the fuel mixtures reduces the maximum soot volume fraction (f_v) in the wing of the flame. Notably, the oxygenated fuels each exhibit a different extent of reduction in the maximum soot volume fraction. The EtOH-Jet A2 flames show the largest decrease in soot volume fraction, followed by the DMC, $PODE_3$ and DMM-Jet A2 flames. It is suggested that this trend is related to the molecular structure of the oxygenated fuels, where the oxygenated functional groups of DMC, $PODE_3$ and DMM are all embedded within their molecular structure. This may reduce the availability of oxygen species to participate in soot reduction reactions. In contrast, the EtOH-Jet A2 flames have the highest reduction in soot volume fraction, possibly because the hydroxyl functional group in EtOH is not embedded within its molecular structure and can produce hydroxyl radicals during the pyrolysis of EtOH in the flame. In EtOH/*n*-pentane premixed flames, for example, the production of hydroxyl radicals increased with the presence of EtOH in the system [40]. These hydroxyl radicals can oxidise soot precursors and soot [31], which consequently reduce the overall soot produced in the flame [28, 86].

The findings are consistent with the comparison of the formation of soot precursors from the combustion of C_2H_6O isomers: ethanol (C_2H_5OH) and dimethyl ether (CH_3OCH_3) [40, 94]. Both were able to reduce the formation of soot precursors in premixed laminar flame [94] and flow reactor [40] due to the increased proportion of oxygenated species in the system [40, 94]. Despite the fact that the C_2H_6O isomers have the same oxygen content, the differences in their oxygen-containing functional groups and hence their fuel-specific destruction pathways were identified to influence the formation of the soot precursors and oxygenated air pollutants [94]. This was also clear where the amount of the soot precursor (benzene) formed in laminar coflow diffusion flames was lower when ethylene was doped with EtOH as opposed to dimethyl ether [64]. Similarly, in mixtures with the same O/C ratio, the $C_4H_{10}O$ isomers diethyl ether and butanol were found to produce soot precursors in laminar premixed low-pressure flames based on the number of C-C bonds and the type of oxygenated functional groups in their molecular structure rather than their oxygen content [92]. The observations show that whilst the reduction in soot volume fraction is broadly correlated with the O/C ratio of fuel blends, the type of oxygenated fuels may also play a significant role in influencing the soot volume fraction in flames.

Figure 7(b) shows the percentage reduction in the average particle size at the tip of the flame versus the oxygen/carbon (O/C) ratio of fuel blends. The reduction in the average particle size at the tip of the flame is broadly correlated with the O/C ratio, however the uncertainties in the measurements are too large to draw any firm conclusions about the differences in behaviour between the different fuels.

3.5 Correlations of soot measurements to oxygen extended sooting index

Figure 8(a) and **(b)** show the maximum soot volume fraction in the wing of the flame and the average particle size at the tip of the flame versus the oxygen extended sooting index (OESI). It is believed that this is the first time that these quantities have been reported.

As shown in Figure 8(a), the maximum soot volume fraction in the wing of the flame for all the oxygenated fuels broadly correlates with the OESI for all the oxygenated fuels. A

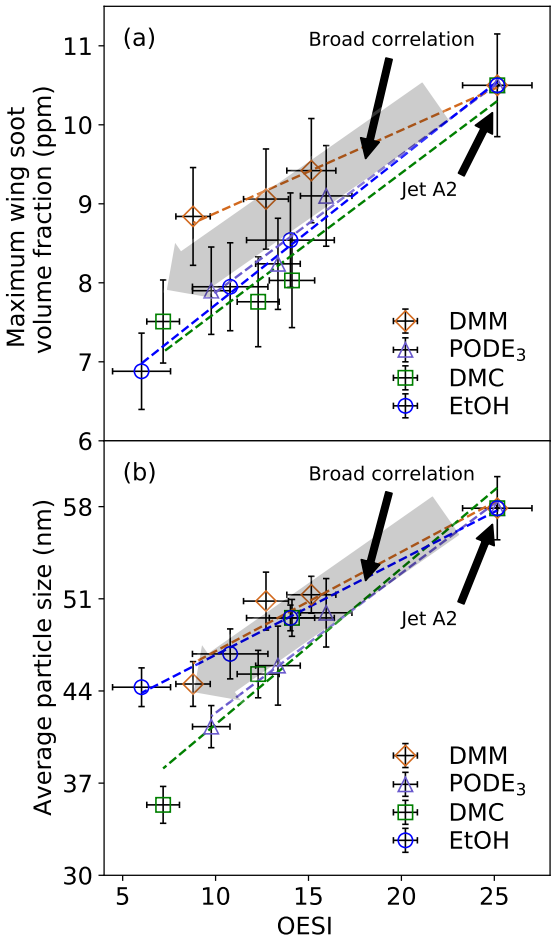

Figure 8: *(a) The maximum soot volume fraction in the wing of the flame and (b) the average particle size at the tip of the flame versus OESI. The error bars are calculated using the error propagation method [96] and show the standard error of five measurements.*

closer inspection of the trends from the figure suggests that there are minute differences between the oxygenated fuels studied. DMM and $PODE_3$ are both poly-ether compounds with different oxygenated fuel oxygen content (42% and 47%, respectively). They exhibit trends that are correlated to their oxygen content, *i.e.* lower oxygen content shows a smaller decrease in maximum soot volume fraction with the decrease in OESI. $PODE_3$, DMC and EtOH have different oxygen-containing functional groups and oxygen content. However, they show a similar decrease in the maximum soot volume fraction with the decrease in OESI. The effect of oxygen content seems to be significant for the poly-ether compounds, but not DMC and EtOH. Nonetheless, OESI showed strong correlation with the maximum soot volume fraction measurements with only small differences between the fuels studied.

The findings are consistent with studies on mono-ethers (DME, DEE and DBE) [92, 95, 97]. The oxygen content of the mono-ethers were varied by changing the number of C-C bonds. The corresponding oxygen content of DME, DEE and DBE are 35%, 22% and

12%, respectively. The mono-ether with the highest oxygen content (DME) produced the least amount of soot precursors, followed by DEE and DBE [97], similar to the trend of the maximum soot volume fraction measurements observed for poly-ethers in the current study. Additionally, in $PODE_3$-blended premixed ethylene/air flame, the oxygen that was embedded within the molecular structure of the $PODE_3$ was found to be effective in reducing the total number of soot precursors and hence the overall amount of soot formed [25].

As shown in Figure 8(b), the average particle size at tip of the flame for all the oxygenated fuel-Jet A2 blends also correlate well with the OESI. However, there are differences between the different fuel blends. The DMM and EtOH-Jet A2 flames show a smaller decrease in average particle size with the decrease in OESI compared with DMC and $PODE_3$-Jet A2 flames. The split is consistent with the observations in Figure 6 and may be linked to the O/C ratio of the oxygenated fuels ($PODE_3$ and DMC at 1.1 and 1.3 versus EtOH and DMM at 0.7 and 0.9, respectively). The correlations observed in Figure 8(b) suggest that OESI can also be useful to correlate average particle size in flames. However, there may also be some dependencies on the O/C ratio of the fuel blend.

4 Conclusions

An ASTM D1322 smoke point lamp was used to investigate the sooting behaviour of oxygenated fuel-Jet A2 blends. Dimethyl carbonate (DMC), dimethoxymethane (DMM), ethanol (EtOH) and polyoxymethylene dimethyl ether 3 ($PODE_3$) were blended with Jet A2 at volumetric percentages up to 20%. The sooting tendency of the fuel mixtures was determined using the smoke point procedure. The soot volume fraction and the particle size distribution (PSD) were measured using colour-ratio pyrometry and differential mobility spectrometry, respectively. The data were analysed to investigate the factors affecting the sooting tendency of oxygenated fuel-Jet A2 blends and to explore the correlations of the PSD and soot volume fraction with OESI.

The addition of the oxygenated fuel in Jet A2 was found to reduce the sooting tendency of the fuel mixtures. The sooting tendency was calculated using the oxygen extended sooting index (OESI). The OESI was found to be negatively correlated with the volumetric percentage, the mole percentage and the oxygen content of the oxygenated fuel-Jet A2 blends, with mole percentage showing a tighter correlation than volumetric percentage. The fuel blends containing EtOH showed a significantly greater reduction in OESI than the other fuel blends when plotted against the oxygen content of the fuel blend, suggesting that oxygen content is insufficient in explaining all of the effect of the oxygenated fuel blend. The molecular structure of the oxygenated fuel is also important, and a marked difference was observed in the behaviour of the fuels with and without carbon-carbon (C-C) bonds.

The soot volume fraction in the wing of the flame and the average particle size at the tip of the flame were analysed versus the oxygen/carbon (O/C) ratio of the fuel mixture. The percentage reduction in soot volume fraction in the wing of the flame was proportional to the O/C ratio of the fuel mixture. The extent of reduction was the largest for EtOH, followed by DMC, $PODE_3$ and DMM. Although EtOH has the lowest O/C ratio, it has a

C-C bond and an non-embedded oxygenated functional group. The effect of this is that the oxygenated functional group (hydroxyl) is more readily accessible to react with soot and soot precursors to promote soot reduction. In the case of DMC, $PODE_3$ and DMM, the oxygen is embedded within the carbon-oxygen-carbon (C-O-C) skeletal structure. This suggests that the reduction in the soot volume fraction in the wing of the flame is also significantly influenced by the molecular structure of the oxygenated fuel. Meanwhile, the percentage reduction in the average particle size at the tip of the flame was found to be broadly proportional to the O/C ratio, but with no discernible differences between the different fuels.

The soot volume fraction in the wing of the flame and the average particle size at the tip of the flame were observed to correlate broadly with the OESI of the fuel mixtures. In the case of the poly-ethers (DMM and $PODE_3$), the soot volume fraction was observed also to depend on their oxygen content. In contrast, average particle size at the tip of the flame was observed also to depend on the O/C ratio of the fuel blend. Although there are slight differences in the correlations between the oxygenated fuels, the broad correlations indicate that the OESI obtained using the smoke point procedure can be used to infer the approximate soot volume fraction and average particle size measured in flames.

In this work, we have demonstrated for the first time that the average particle size and the soot volume fraction (measured with an easily implemented technique such as colour-ratio pyrometry) can be determined via correlations with the sooting tendency measurements. This is significant because the aviation industry can use these correlations to support the evaluation of the capability of new Sustainable Aviation Fuel blends to meet the particulate matter standards that will be introduced by regulators in the coming future.

Research data

The flame pyrometry code supporting this publication is available in the University of Cambridge data repository (doi:10.17863/CAM.36025) and also on GitHub (`www.github.com/ucam-ceb-como/FlamePyrometry`).

Acknowledgements

This research was supported by the National Research Foundation, Prime Minister's Office, Singapore under its Campus for Research Excellence and Technological Enterprise (CREATE) programme. Y. R. Tan acknowledges financial support provided by Fitzwilliam College Cambridge, Trinity College Cambridge and the Cambridge Trust. M. Kraft gratefully acknowledges the support of the Alexander von Humboldt Foundation. The authors would also like to thank Savvas Gkantonas, Roberto Ciardiello and Professor Epaminondas Mastorakos from the Department of Engineering at University of Cambridge for the procurement of the Jet A2 (POSF 10325) used in the current investigation.

A Supplementary materials

A1.1 Smoke point measurements of fuel blends

Table A1.1: *Smoke point of pure fuels and fuel mixtures at different volumetric blends with Jet Fuel A-2.*

Fuel	Smoke point (mm)			
	5 vol.%	10 vol.%	20 vol.%	100 vol.%
Dimethyl carbonate	26.7	27.0	30.7	-
Dimethoxymethane	26.0	26.2	29.5	-
PODE$_3$	25.8	27.8	31.2	-
Ethanol	26.1	27.4	30.3	-
Jet Fuel A-2	-	-	-	25.0
1-Methylnapthalene	-	-	-	5.2
n-Heptane	-	-	-	62.3
Decane	-	-	-	51.6
Toluene	-	-	-	8.6
Cyclohexane	-	-	-	28.8
Dodecane	-	-	-	43.0

A1.2 Fuel consumption rates

Table A1.2 shows the rate of fuel consumption for flame studied with their flame lengths maintained at about 24.5 mm. The rate of fuel consumption is obtained from the measurements of the change in the mass of fuel in the smoke point lamp. Each measurement was performed over 16 minutes.

Table A1.2: *Rate of fuel consumption for the flames studied.*

Fuel	Fuel consumption (mg/s)			
	5 vol.%	10 vol.%	20 vol.%	100 vol.%
Jet Fuel A-2	-	-	-	1.04
Dimethyl carbonate	1.06	1.10	1.05	-
Dimethoxymethane	0.98	1.03	1.00	-
PODE$_3$	1.07	1.06	1.10	-
Ethanol	1.05	1.00	0.94	-

References

[1] A. O. G. Abdalla and D. Liu. Dimethyl carbonate as a promising oxygenated fuel for combustion: A review. *Energies*, 11(6):1–20, 2018. doi:10.3390/en11061552.

[2] M. K. Abdrabou, P. P. Morajkar, G. D. J. Guerrero Peña, A. Raj, M. Elkadi, and A. V. Salkar. Effect of 5-membered bicyclic hydrocarbon additives on nanostructural disorder and oxidative reactivity of diffusion flame-generated diesel soot. *Fuel*, 275:117918, 2020. doi:10.1016/j.fuel.2020.117918.

[3] M. I. Apostolopoulos, M. I. Taroudakis, and D. G. Papazoglou. Application of inverse Abel techniques in in-line holographic microscopy. *Optics Communications*, 296:25–34, 2013. doi:10.1016/j.optcom.2013.01.053.

[4] ASTM International. D1322-19 standard test method for smoke point of kerosene and aviation turbine fuel, 2019.

[5] ASTM International. D7566-20b standard specification for aviation turbine fuel containing synthesized hydrocarbons, 2020.

[6] O. I. Awad, X. Ma, M. Kamil, O. M. Ali, Y. Ma, and S. Shuai. Overview of polyoxymethylene dimethyl ether additive as an eco-friendly fuel for an internal combustion engine: Current application and environmental impacts. *Science of The Total Environment*, 715:136849, 2020. doi:10.1016/j.scitotenv.2020.136849.

[7] E. J. Barrientos, M. Lapuerta, and A. L. Boehman. Group additivity in soot formation for the example of C-5 oxygenated hydrocarbon fuels. *Combustion and Flame*, 160(8):1484–1498, 2013. doi:10.1016/j.combustflame.2013.02.024.

[8] D. L. Bartholet, M. A. Arellano-Treviño, F. L. Chan, S. Lucas, J. Zhu, P. C. St. John, T. L. Alleman, C. S. McEnally, L. D. Pfefferle, D. A. Ruddy, B. Windom, T. D. Foust, and K. F. Reardon. Property predictions demonstrate that structural diversity can improve the performance of polyoxymethylene ethers as potential bio-based diesel fuels. *Fuel*, 295:120509, 2021. doi:10.1016/j.fuel.2021.120509.

[9] A. M. Boies, M. E. J. Stettler, J. J. Swanson, T. J. Johnson, J. S. Olfert, M. Johnson, M. L. Eggersdorfer, T. Rindlisbacher, J. Wang, K. Thomson, G. Smallwood, Y. Sevcenco, D. Walters, P. I. Williams, J. Corbin, A. A. Mensah, J. Symonds, R. Dastanpour, and S. N. Rogak. Particle emission characteristics of a gas turbine with a double annular combustor. *Aerosol Science and Technology*, 49(9):842–855, 2015. doi:10.1080/02786826.2015.1078452.

[10] M. L. Botero, S. Mosbach, and M. Kraft. Sooting tendency of paraffin components of diesel and gasoline in diffusion flames. *Fuel*, 126:8–15, 2014. doi:10.1016/j.fuel.2014.02.005.

[11] M. L. Botero, S. Mosbach, J. Akroyd, and M. Kraft. Sooting tendency of surrogates for the aromatic fractions of diesel and gasoline in a wick-fed diffusion flame. *Fuel*, 153:31–39, 2015. doi:10.1016/j.fuel.2015.02.108.

[12] M. L. Botero, S. Mosbach, and M. Kraft. Sooting tendency and particle size distributions of n-heptane/toluene mixtures burned in a wick-fed diffusion flame. *Fuel*, 169:111–119, 2016. doi:10.1016/j.fuel.2015.12.014.

[13] H. F. Calcote and D. M. Manos. Effect of molecular structure on incipient soot formation. *Combustion and Flame*, 49(1):289–304, 1983. doi:10.1016/0010-2180(83)90172-4.

[14] M. Chen and D. Liu. Morphology and nanostructure transitions of soot with various dimethyl ether additions in nonpremixed ethylene flames at different scales. *Energy & Fuels*, 34(12):16705–16719, 2020. doi:10.1021/acs.energyfuels.0c03305.

[15] C. T. Chong, B. Tian, J.-H. Ng, L. Fan, S. Ni, K. Y. Wong, and S. Hochgreb. Quantification of carbon particulates produced under open liquid pool and prevaporised flame conditions: Waste cooking oil biodiesel and diesel blends. *Fuel*, 270:117469, 2020. doi:10.1016/j.fuel.2020.117469.

[16] M. Colket, J. Heyne, M. Rumizen, M. Gupta, T. Edwards, W. M. Roquemore, G. Andac, R. Boehm, J. Lovett, R. Williams, J. Condevaux, D. Turner, N. Rizk, J. Tishkoff, C. Li, J. Moder, D. Friend, and V. Sankaran. Overview of the national jet fuels combustion program. *AIAA Journal*, 55(4):1087–1104, 2017. doi:10.2514/1.J055361.

[17] E. Corsini, M. Marinovich, and R. Vecchi. Ultrafine particles from residential biomass combustion: A review on experimental data and toxicological response. *International Journal of Molecular Sciences*, 20(20):4992, 2019. doi:10.3390/ijms20204992.

[18] J. A. H. Dreyer, R. Slavchov, and A. Menon. FLiPPID flame pyrometry python code. *Apollo*, 2019. doi:10.17863/CAM.36025.

[19] J. A. H. Dreyer, R. I. Slavchov, E. J. Rees, J. Akroyd, M. Salamanca, S. Mosbach, and M. Kraft. Improved methodology for performing the inverse Abel transform of flame images for color ratio pyrometry. *Applied Optics*, 58(10):2662–2670, Apr 2019. doi:10.1364/AO.58.002662.

[20] V. Dribinski, A. Ossadtchi, V. A. Mandelshtam, and H. Reisler. Reconstruction of Abel-transformable images: The gaussian basis-set expansion Abel transform method. *Review of Scientific Instruments*, 73(7):2634–2642, 2002. doi:10.1063/1.1482156.

[21] L. H. Duong, I. K. Reksowardojo, T. H. Soerawidjaja, D. N. Pham, and O. Fujita. The sooting tendency of aviation biofuels and jet range paraffins: effects of adding aromatics, carbon chain length of normal paraffins, and fraction of branched paraffins. *Combustion Science and Technology*, 190(10):1710–1721, 2018. doi:10.1080/00102202.2018.1468323.

[22] E. F. Durand, A. P. Crayford, and M. Johnson. Experimental validation of thermophoretic and bend nanoparticle loss for a regulatory prescribed aircraft nvpm

sampling system. *Aerosol Science and Technology*, 54(9):1019–1033, 2020. doi:10.1080/02786826.2020.1756212.

[23] J. T. Edwards. *Reference Jet Fuels for Combustion Testing*, pages 1–58. American Institute of Aeronautics and Astronautics, 2017. doi:10.2514/6.2017-0146.

[24] J. Fang, Y. Liu, K. Wang, H. R. Shah, S. Mu, X. Lang, and J. Wang. Sooting tendency analysis of oxygenate-diesel blended fuels by the affecting indicators of carbon number, oxygen content and h/c ratio. *Fuel*, 290:119789, 2021. doi:10.1016/j.fuel.2020.119789.

[25] F. Ferraro, C. Russo, R. Schmitz, C. Hasse, and M. Sirignano. Experimental and numerical study on the effect of oxymethylene ether-3 (OME3) on soot particle formation. *Fuel*, 286:119353, 2021. doi:10.1016/j.fuel.2020.119353.

[26] P. L. Feuvre. International Energy Agency, Are aviation biofuels ready for take off?, 2019. URL https://www.iea.org/commentaries/are-aviation-biofuels-ready-for-take-off. Last accessed 16 November 2020.

[27] P. L. Feuvre. International Energy Agency, Transport biofuels, 2020. URL https://www.iea.org/reports/transport-biofuels. Last accessed 17 November 2020.

[28] M. Frenklach. Reaction mechanism of soot formation in flames. *Physical Chemistry Chemical Physics*, 4:2028–2037, 2002. doi:10.1039/B110045A.

[29] I. Frenzel, H. Krause, and D. Trimis. Study on the influence of ethanol and butanol addition on soot formation in iso-octane flames. *Energy Procedia*, 120:721–728, 2017. doi:10.1016/j.egypro.2017.07.203.

[30] H. Ghiassi, P. Toth, and J. S. Lighty. Sooting behaviors of n-butanol and n-dodecane blends. *Combustion and Flame*, 161(3):671–679, 2014. doi:10.1016/j.combustflame.2013.10.011.

[31] H. Ghiassi, D. Lignell, and J. S. Lighty. Soot oxidation by OH: Theory development, model, and experimental validation. *Energy & Fuels*, 31(3):2236–2245, 2017. doi:10.1021/acs.energyfuels.6b02193.

[32] A. Gómez, J. Soriano, and O. Armas. Evaluation of sooting tendency of different oxygenated and paraffinic fuels blended with diesel fuel. *Fuel*, 184:536–543, 2016. doi:10.1016/j.fuel.2016.07.049.

[33] A. Gómez, R. García-Contreras, J. Soriano, and C. Mata. Comparative study of the opacity tendency of alternative diesel fuels blended with gasoline. *Fuel*, 264: 116860, 2020. doi:10.1016/j.fuel.2019.116860.

[34] J. Holladay, Z. Abdullah, and J. Heyne. US Department of Energy, sustainable aviation fuel: Review of technical pathways, 2020. URL https://www.energy.gov/sites/prod/files/2020/09/f78/beto-sust-aviation-fuel-sep-2020.pdf. Last accessed 16 April 2021.

[35] X. Hui, W. Liu, X. Xue, and C.-J. Sung. Sooting characteristics of hydrocarbon compounds and their blends relevant to aviation fuel applications. *Fuel*, 287: 119522, 2021. doi:10.1016/j.fuel.2020.119522.

[36] ICAO Vision. Declaration of the second conference on aviation and alternative fuels, 2017. URL https://www.icao.int/environmental-protection/GFAAF/pages/ICAO-Vision.aspx. Last accessed 17 November 2020.

[37] I. C. Jaramillo, A. Sturrock, H. Ghiassi, D. J. Woller, C. E. Deering-Rice, J. S. Lighty, R. Paine, C. Reilly, and K. E. Kelly. Effects of fuel components and combustion particle physicochemical properties on toxicological responses of lung cells. *Journal of Environmental Science and Health, Part A*, 53(4):295–309, 2018. doi:10.1080/10934529.2017.1400793.

[38] Q. Jiao, J. E. Anderson, T. J. Wallington, and E. M. Kurtz. Smoke point measurements of diesel-range hydrocarbon–oxygenate blends using a novel approach for fuel blend selection. *Energy & Fuels*, 29(11):7641–7649, 2015. doi:10.1021/acs.energyfuels.5b01624.

[39] C. Jin, X. Zhang, X. Wang, Y. Xiang, X. Cui, Z. Yin, X. Sun, J. Ji, G. Wang, and H. Liu. Effects of polyoxymethylene dimethyl ethers on the solubility of ethanol/diesel and hydrous ethanol/diesel fuel blends. *Energy Science & Engineering*, 7(6):2855–2865, 2019. doi:10.1002/ese3.466.

[40] H. Jin, J. Pieper, C. Hemken, E. Bräuer, L. Ruwe, and K. Kohse-Höinghaus. Chemical interaction of dual-fuel mixtures in low-temperature oxidation, comparing n-pentane/dimethyl ether and n-pentane/ethanol. *Combustion and Flame*, 193:36–53, 2018. doi:10.1016/j.combustflame.2018.03.003.

[41] W. Junkermann, B. Vogel, and M. A. Sutton. The climate penalty for clean fossil fuel combustion. *Atmospheric Chemistry and Physics*, 11(24):12917–12924, 2011. doi:10.5194/acp-11-12917-2011.

[42] Y. Kang, Y. Sun, X. Lu, X. Gou, S. Sun, J. Yan, Y. Song, P. Zhang, Q. Wang, and X. Ji. Soot formation characteristics of ethylene premixed burner-stabilized stagnation flame with dimethyl ether addition. *Energy*, 150:709–721, 2018. doi:10.1016/j.energy.2018.03.025.

[43] T. Kasper, P. Oßwald, U. Struckmeier, K. Kohse-Höinghaus, C. A. Taatjes, J. Wang, T. A. Cool, M. E. Law, A. Morel, and P. R. Westmoreland. Combustion chemistry of the propanol isomers — investigated by electron ionization and VUV-photoionization molecular-beam mass spectrometry. *Combustion and Flame*, 156 (6):1181–1201, 2009. doi:10.1016/j.combustflame.2009.01.023.

[44] N. J. Kempema and M. B. Long. Effect of soot self-absorption on color-ratio pyrometry in laminar coflow diffusion flames. *Optics Letters*, 43(5):1103–1106, 2018. doi:10.1364/OL.43.001103.

[45] M. R. Kholghy, J. Weingarten, A. D. Sediako, J. Barba, M. Lapuerta, and M. J. Thomson. Structural effects of biodiesel on soot formation in a laminar coflow diffusion flame. *Proceedings of the Combustion Institute*, 36(1):1321–1328, 2017. doi:10.1016/j.proci.2016.06.119.

[46] A. Khosousi, F. Liu, S. B. Dworkin, N. A. Eaves, M. J. Thomson, X. He, Y. Dai, Y. Gao, F. Liu, S. Shuai, and J. Wang. Experimental and numerical study of soot formation in laminar coflow diffusion flames of gasoline/ethanol blends. *Combustion and Flame*, 162(10):3925–3933, 2015. doi:10.1016/j.combustflame.2015.07.029.

[47] K. Kohse-Höinghaus. Clean combustion: Chemistry and diagnostics for a systems approach in transportation and energy conversion. *Progress in Energy and Combustion Science*, 65:1–5, 2018. doi:10.1016/j.pecs.2017.10.001.

[48] K. Kohse-Höinghaus. A new era for combustion research. *Pure and Applied Chemistry*, 91(2):271–288, 2019. doi:10.1515/pac-2018-0608.

[49] K. Kohse-Höinghaus. Combustion in the future: The importance of chemistry. *Proceedings of the Combustion Institute*, 38(1):1–56, 2021. doi:10.1016/j.proci.2020.06.375.

[50] K. Kohse-Höinghaus, P. Oßwald, T. A. Cool, T. Kasper, N. Hansen, F. Qi, C. K. Westbrook, and P. R. Westmoreland. Biofuel combustion chemistry: From ethanol to biodiesel. *Angewandte Chemie International Edition*, 49(21):3572–3597, 2010. doi:10.1002/anie.200905335.

[51] P. B. Kuhn, B. Ma, B. C. Connelly, M. D. Smooke, and M. B. Long. Soot and thin-filament pyrometry using a color digital camera. *Proceedings of the Combustion Institute*, 33(1):743–750, 2011. doi:10.1016/j.proci.2010.05.006.

[52] R. R. Kumal, J. Liu, A. Gharpure, R. L. Vander Wal, J. S. Kinsey, B. Giannelli, J. Stevens, C. Leggett, R. Howard, M. Forde, A. Zelenyuk, K. Suski, G. Payne, J. Manin, W. Bachalo, R. Frazee, T. B. Onasch, A. Freedman, D. B. Kittelson, and J. J. Swanson. Impact of biofuel blends on black carbon emissions from a gas turbine engine. *Energy & Fuels*, 34(4):4958–4966, 2020. doi:10.1021/acs.energyfuels.0c00094.

[53] H.-S. Kwon, M. H. Ryu, and C. Carlsten. Ultrafine particles: unique physicochemical properties relevant to health and disease. *Experimental & Molecular Medicine*, 52(3):318–328, 2020. doi:10.1038/s12276-020-0405-1.

[54] D. S. Lee, D. W. Fahey, A. Skowron, M. R. Allen, U. Burkhardt, Q. Chen, S. J. Doherty, S. Freeman, P. M. Forster, J. Fuglestvedt, A. Gettelman, R. De León, L. L. Lim, M. Lund, R. Millar, B. Owen, J. E. Penner, G. Pitari, M. Prather, R. Sausen, and L. J. Wilcox. The contribution of global aviation to anthropogenic climate forcing for 2000 to 2018. *Atmospheric Environment*, 244:117834, 2021. doi:10.1016/j.atmosenv.2020.117834.

[55] D. Li, W. Fang, Y. Xing, Y. Guo, and R. Lin. Effects of dimethyl or diethyl carbonate as an additive on volatility and flash point of an aviation fuel. *Journal of Hazardous Materials*, 161(2):1193–1201, 2009. doi:10.1016/j.jhazmat.2008.04.070.

[56] F. Liu, X. He, X. Ma, Q. Zhang, M. Thomson, H. Guo, G. Smallwood, S. Shuai, and J. Wang. An experimental and numerical study of the effects of dimethyl ether addition to fuel on polycyclic aromatic hydrocarbon and soot formation in laminar coflow ethylene/air diffusion flames. *Combustion and Flame*, 158(3):547–563, 2011. doi:10.1016/j.combustflame.2010.10.005.

[57] F. Liu, Y. Hua, H. Wu, X. He, and N. Kang. Effect of ethanol addition on soot formation of gasoline in laminar diffusion flames. *SAE International, International Powertrains, Fuels & Lubricants Meeting*, 1:2396, 2017. doi:10.4271/2017-01-2396.

[58] H. Liu, Z. Wang, J. Zhang, J. Wang, and S. Shuai. Study on combustion and emission characteristics of polyoxymethylene dimethyl ethers/diesel blends in light-duty and heavy-duty diesel engines. *Applied Energy*, 185:1393–1402, 2017. doi:10.1016/j.apenergy.2015.10.183.

[59] H. Liu, Z. Wang, Y. Li, Y. Zheng, T. He, and J. Wang. Recent progress in the application in compression ignition engines and the synthesis technologies of polyoxymethylene dimethyl ethers. *Applied Energy*, 233-234:599–611, 2019. doi:10.1016/j.apenergy.2018.10.064.

[60] J. Luo, Y. Zhang, Q. Zhang, J. Liu, and J. Wang. Evaluation of sooting tendency of acetone–butanol–ethanol (ABE) fuels blended with diesel fuel. *Fuel*, 209:394–401, 2017. doi:10.1016/j.fuel.2017.08.019.

[61] C. Magazzino, M. Mele, and N. Schneider. The relationship between air pollution and COVID-19-related deaths: An application to three French cities. *Applied Energy*, 279:115835, 2020. doi:10.1016/j.apenergy.2020.115835.

[62] F. Mahrt, K. Kilchhofer, C. Marcolli, P. Grönquist, R. O. David, M. Rösch, U. Lohmann, and Z. A. Kanji. The impact of cloud processing on the ice nucleation abilities of soot particles at cirrus temperatures. *Journal of Geophysical Research: Atmospheres*, 125(3):1–23, 2020. doi:10.1029/2019JD030922.

[63] L. Malorni, V. Guida, M. Sirignano, G. Genovese, C. Petrarca, and P. Pedata. Exposure to sub-10nm particles emitted from a biodiesel-fueled diesel engine: In vitro toxicity and inflammatory potential. *Toxicology Letters*, 270:51–61, 2017. doi:10.1016/j.toxlet.2017.02.009.

[64] C. S. McEnally and L. D. Pfefferle. The effects of dimethyl ether and ethanol on benzene and soot formation in ethylene nonpremixed flames. *Proceedings of the Combustion Institute*, 31(1):603–610, 2007. doi:10.1016/j.proci.2006.07.005.

[65] C. S. McEnally and L. D. Pfefferle. Sooting tendencies of oxygenated hydrocarbons in laboratory-scale flames. *Environmental Science & Technology*, 45(6): 2498–2503, 2011. doi:10.1021/es103733q.

[66] W. Merchan-Merchan, S. G. Sanmiguel, and S. McCollam. Analysis of soot particles derived from biodiesels and diesel fuel air-flames. *Fuel*, 102:525–535, 2012. doi:10.1016/j.fuel.2012.04.029.

[67] R. Moore, K. Thornhill, B. Weinzierl, D. Sauer, E. D'Ascoli, J. Kim, M. Lichtenstern, M. Scheibe, B. Beaton, A. J. Beyersdorf, J. Barrick, D. Bulzan, C. A. Corr, E. Crosbie, T. Jurkat, R. Martin, D. Riddick, M. Shook, G. Slover, C. Voigt, R. White, E. Winstead, R. Yasky, L. D. Ziemba, A. Brown, H. Schlager, and B. E. Anderson. Biofuel blending reduces particle emissions from aircraft engines at cruise conditions. *Nature*, 543:411–415, 2017. doi:10.1038/nature21420.

[68] P. P. Morajkar, M. K. Abdrabou, A. V. Salkar, A. Raj, M. Elkadi, and D. H. Anjum. Nanostructural disorder and reactivity comparison of flame soot and engine soot using diesel and Jatropha biodiesel/diesel blend as fuels. *Energy & Fuels*, 34(10): 12960–12971, 2020. doi:10.1021/acs.energyfuels.0c02063.

[69] D. B. Olson, J. C. Pickens, and R. J. Gill. The effects of molecular structure on soot formation II. diffusion flames. *Combustion and Flame*, 62(1):43–60, 1985. doi:10.1016/0010-2180(85)90092-6.

[70] P. Oßwald, H. Güldenberg, K. Kohse-Höinghaus, B. Yang, T. Yuan, and F. Qi. Combustion of butanol isomers – a detailed molecular beam mass spectrometry investigation of their flame chemistry. *Combustion and Flame*, 158(1):2–15, 2011. doi:10.1016/j.combustflame.2010.06.003.

[71] J. O'Malley, N. Pavlenko, and S. Searle. Estimating sustainable aviation fuel feedstock availability to meet growing European Union demand, 2021. URL https://theicct.org/sites/default/files/publications/Sustainable-aviation-fuel-feedstock-eu-mar2021.pdf. Last accessed 21 April 2021.

[72] R. S. Pathania, A. W. Skiba, R. Ciardiello, and E. Mastorakos. Blow-off mechanisms of turbulent premixed bluff-body stabilised flames operated with vapourised kerosene fuels. *Proceedings of the Combustion Institute*, 38(2):2957–2965, 2021. doi:10.1016/j.proci.2020.06.213.

[73] P. Pepiot-Desjardins, H. Pitsch, R. Malhotra, S. Kirby, and A. Boehman. Structural group analysis for soot reduction tendency of oxygenated fuels. *Combustion and Flame*, 154(1):191–205, 2008. doi:10.1016/j.combustflame.2008.03.017.

[74] W. Raillant-Clark. ICAO council adopts important environmental standard, 2020. URL https://www.icao.int/Newsroom/Pages/ICAO-Council-adopts-important-environmental-standard.aspx. Last accessed 9 April 2021.

[75] G. Rubio-Gomez, L. Corral-Gomez, J. A. Soriano, A. Gómez, and F. J. Castillo-Garcia. Vision based algorithm for automated determination of smoke point of diesel blends. *Fuel*, 235:595–602, 2019. doi:10.1016/j.fuel.2018.08.032.

[76] C. Russo, A. D'Anna, A. Ciajolo, and M. Sirignano. The effect of butanol isomers on the formation of carbon particulate matter in fuel-rich

premixed ethylene flames. *Combustion and Flame*, 199:122–130, 2019. doi:10.1016/j.combustflame.2018.10.025.

[77] M. Salamanca, M. Sirignano, M. Commodo, P. Minutolo, and A. D'Anna. The effect of ethanol on the particle size distributions in ethylene premixed flames. *Experimental Thermal and Fluid Science*, 43:71–75, 2012. doi:10.1016/j.expthermflusci.2012.04.006.

[78] M. Salamanca, M. Sirignano, and A. D'Anna. Particulate formation in premixed and counter-flow diffusion ethylene/ethanol flames. *Energy & Fuels*, 26(10):6144–6152, 2012. doi:10.1021/ef301081q.

[79] S. M. Sarathy, S. Vranckx, K. Yasunaga, M. Mehl, P. Oßwald, W. K. Metcalfe, C. K. Westbrook, W. J. Pitz, K. Kohse-Höinghaus, R. X. Fernandes, and H. J. Curran. A comprehensive chemical kinetic combustion model for the four butanol isomers. *Combustion and Flame*, 159(6):2028–2055, 2012. doi:10.1016/j.combustflame.2011.12.017.

[80] S. M. Sarathy, P. Oßwald, N. Hansen, and K. Kohse-Höinghaus. Alcohol combustion chemistry. *Progress in Energy and Combustion Science*, 44:40–102, 2014. doi:10.1016/j.pecs.2014.04.003.

[81] D. E. Schraufnagel. The health effects of ultrafine particles. *Experimental & Molecular Medicine*, 52:311–317, 2020. doi:10.1038/s12276-020-0403-3.

[82] M. Sirignano, A. Ciajolo, A. D'Anna, and C. Russo. Chemical features of particles generated in an ethylene/ethanol premixed flame. *Energy & Fuels*, 31(3):2370–2377, 2017. doi:10.1021/acs.energyfuels.6b02372.

[83] M. D. Smooke, M. B. Long, B. C. Connelly, M. B. Colket, and R. J. Hall. Soot formation in laminar diffusion flames. *Combustion and Flame*, 143(4):613–628, 2005. doi:10.1016/j.combustflame.2005.08.028.

[84] A. Srivastava. COVID-19 and air pollution and meteorology-an intricate relationship: A review. *Chemosphere*, 263:128297, 2021. doi:10.1016/j.chemosphere.2020.128297.

[85] W. Sun, B. Yang, N. Hansen, C. K. Westbrook, F. Zhang, G. Wang, K. Moshammer, and C. K. Law. An experimental and kinetic modeling study on dimethyl carbonate (DMC) pyrolysis and combustion. *Combustion and Flame*, 164:224–238, 2016. doi:10.1016/j.combustflame.2015.11.019.

[86] Z. Sun, B. Dally, Z. Alwahabi, and G. Nathan. The effect of oxygen concentration in the co-flow of laminar ethylene diffusion flames. *Combustion and Flame*, 211: 96–111, 2020. doi:10.1016/j.combustflame.2019.09.023.

[87] Y. R. Tan, M. L. Botero, Y. Sheng, J. A. H. Dreyer, R. Xu, W. Yang, and M. Kraft. Sooting characteristics of polyoxymethylene dimethyl ether blends with diesel in a diffusion flame. *Fuel*, 224:499–506, 2018. doi:10.1016/j.fuel.2018.03.051.

[88] Y. R. Tan, M. Salamanca, J. Bai, J. Akroyd, and M. Kraft. Structural effects of C3 oxygenated fuels on soot formation in ethylene coflow diffusion flames. *Combustion and Flame*, 232:111512, 2021. doi:10.1016/j.combustflame.2021.111512.

[89] Y. R. Tan, M. Salamanca, L. Pascazio, J. Akroyd, and M. Kraft. The effect of poly(oxymethylene) dimethyl ethers ($PODE_3$) on soot formation in ethylene/$PODE_3$ laminar coflow diffusion flames. *Fuel*, 283:118769, 2021. doi:10.1016/j.fuel.2020.118769.

[90] J. Teter, P. L. Feuvre, P. Bains, and L. L. Re. International Energy Agency, Aviation, 2020. URL https://www.iea.org/reports/aviation. Last accessed 16 November 2020.

[91] C. Togbé, L.-S. Tran, D. Liu, D. Felsmann, P. Oßwald, P.-A. Glaude, B. Sirjean, R. Fournet, F. Battin-Leclerc, and K. Kohse-Höinghaus. Combustion chemistry and flame structure of furan group biofuels using molecular-beam mass spectrometry and gas chromatography – part III: 2,5-dimethylfuran. *Combustion and Flame*, 161 (3):780–797, 2014. doi:10.1016/j.combustflame.2013.05.026.

[92] L.-S. Tran, J. Pieper, M. Zeng, Y. Li, X. Zhang, W. Li, I. Graf, F. Qi, and K. Kohse-Höinghaus. Influence of the biofuel isomers diethyl ether and n-butanol on flame structure and pollutant formation in premixed n-butane flames. *Combustion and Flame*, 175:47–59, 2017. doi:10.1016/j.combustflame.2016.06.031.

[93] M. K. Tran, D. Dunn-Rankin, and T. K. Pham. Characterizing sooting propensity in biofuel–diesel flames. *Combustion and Flame*, 159(6):2181–2191, 2012. doi:10.1016/j.combustflame.2012.01.008.

[94] J. Wang, U. Struckmeier, B. Yang, T. A. Cool, P. Oßwald, K. Kohse-Höinghaus, T. Kasper, N. Hansen, and P. R. Westmoreland. Isomer-specific influences on the composition of reaction intermediates in dimethyl ether/propene and ethanol/propene flame. *The Journal of Physical Chemistry A*, 112(39):9255–9265, 2008. doi:10.1021/jp8011188.

[95] Z. Wang, X. Zhang, L. Xing, L. Zhang, F. Herrmann, K. Moshammer, F. Qi, and K. Kohse-Höinghaus. Experimental and kinetic modeling study of the low- and intermediate-temperature oxidation of dimethyl ether. *Combustion and Flame*, 162 (4):1113–1125, 2015. doi:10.1016/j.combustflame.2014.10.003.

[96] R. J. Watson, M. L. Botero, C. J. Ness, N. M. Morgan, and M. Kraft. An improved methodology for determining threshold sooting indices from smoke point lamps. *Fuel*, 111:120–130, 2013. doi:10.1016/j.fuel.2013.04.024.

[97] J. Wullenkord, L.-S. Tran, J. Böttchers, I. Graf, and K. Kohse-Höinghaus. A laminar flame study on di-n-butyl ether as a potential biofuel candidate. *Combustion and Flame*, 190:36–49, 2018. doi:10.1016/j.combustflame.2017.11.006.

[98] J. Wullenkord, I. Graf, M. Baroncelli, D. Felsmann, L. Cai, H. Pitsch, and K. Kohse-Höinghaus. Laminar premixed and non-premixed flame investigation

on the influence of dimethyl ether addition on n-heptane combustion. *Combustion and Flame*, 212:323–336, 2020. doi:10.1016/j.combustflame.2019.11.012.

[99] M. Yahyaoui, I. Lombaert-Valot, G. Mignani, and N. Perret. Dialkyl carbonate compounds as anti-soot additives for aviation fuel, WIPO (PCT) WO 2017/129726 Al, 2017.

[100] F. Yan, L. Xu, Y. Wang, S. Park, S. M. Sarathy, and S. H. Chung. On the opposing effects of methanol and ethanol addition on PAH and soot formation in ethylene counterflow diffusion flames. *Combustion and Flame*, 202:228–242, 2019. doi:10.1016/j.combustflame.2019.01.020.

[101] S. Yan, E. G. Eddings, A. B. Palotas, R. J. Pugmire, and A. F. Sarofim. Prediction of sooting tendency for hydrocarbon liquids in diffusion flames. *Energy & Fuels*, 19(6):2408–2415, 2005. doi:10.1021/ef050107d.

[102] J. Yang, Z. Xin, Q. S. He, K. Corscadden, and H. Niu. An overview on performance characteristics of bio-jet fuels. *Fuel*, 237:916–936, 2019. doi:10.1016/j.fuel.2018.10.079.

[103] X. Zhang, M. Tang, F. Guo, F. Wei, Z. Yu, K. Gao, M. Jin, J. Wang, and K. Chen. Associations between air pollution and COVID-19 epidemic during quarantine period in china. *Environmental Pollution*, 268:115897, 2021. doi:10.1016/j.envpol.2020.115897.

[104] Y. Zhang, Y. Li, P. Liu, R. Zhan, Z. Huang, and H. Lin. Investigation on the chemical effects of dimethyl ether and ethanol additions on pah formation in laminar premixed ethylene flames. *Fuel*, 256:115809, 2019. doi:10.1016/j.fuel.2019.115809.